15th World Congress on Computational Mechanics (WCCM-XV)
8th Asian Pacific Congress on Computational Mechanics (APCOM-VIII)
Virtual Congress: 31 July – 5 August 2022
S. Koshizuka (Ed.)

EXTRACTION OF DISASTER AREA FROM SATELLITE IMAGE BY COMBINING MACHINE LEARNING AND IMAGE PROCESSING TECHNOLOGY

DAIKI SENO[1], SHIORI KUBO[2], CHIKAKO ISOUCHI[3] AND HIDENORI YOSHIDA[4]

[1]Graduate School of Engineering, Kagawa University,
2217-20 Hayashi-cho, Takamatsu, Kagawa, 761-0396,
s21g404@kagawa-u.ac.jp

[2]Institute of Industrial Science, The University of Tokyo,
5-1-5 Kashiwanoha, Kashiwa, Chiba, 277-8574,
Shiori_kubo@metall.t.u-tokyo.ac.jp

[3]Institute of Education, Research and Regional Cooperation
for Crisis Management Shikoku, Kagawa University,
1-1 Saiwai-cho, Takamatsu, Kagawa, 760-8521,
Isouchi.chikako@kagawa-u.ac.jp

[4]Faculty of Engineering and Design, Kagawa University,
2217-20 Hayashi-cho, Takamatsu, Kagawa, 761-0396,
yoshida.hidenori@kagawa-u.ac.jp

Key words: Satellite Image, Machine Learning, Land Cover Classification, Additive Color Mixture

Abstract. *In recent years, heavy rain which frequently occurred in various places in Japan have been caused severe damage. It is important to identify the damaged area for disaster recovery and reconstruction. In this study, we focus on the optical satellite images that are easy to process and interpret, and extract the damaged area by combining a land cover classification method using machine learning and an additive color mixture method. As the results, it is possible to visually express the land cover changes before and after the disasters in a specific category and to extract the damaged area from the optical satellite image.*

1 INTRODUCTION

In recent years, heavy rain which frequently occurred in various places in Japan have been caused severe damages. The average temperature in Japan is increasing at a rate of 1.19°C per 100 years, and the annual frequency of intense rainfall (80 mm or more per one hour), the highest rank in the index indicating rainfall intensity in Japan, is also increasing. Therefore, there is a high possibility that more large-scale water-related disasters will occur in the future. In such a situation, it is necessary to promptly recovery and reconstruction from water-related disasters. In particular, "2018 Japan Floods" is a representative example of a heavy rain in Japan.

This heavy rain brought about the damage due to multiple factors such as inland inundation, sediment run-off and flood inundation. A large number of human resources for disaster response were required, and it was also difficult to fly a helicopter due to the weather. As a result, the problem that it took a long time to grasp the disaster situation, and that recovery and reconstruction were difficult are mentioned. Therefore, it is important to identify a wide range of damaged areas for recovery and reconstruction.

Images taken by unmanned aerial vehicles such as drones and satellite images are often used to grasp the damaged areas. The advantages of drone image are that it allows a rapid response from the occurrence of a disaster to image. However, since images can only be taken over a localized area, it takes time to grasp the situation over a wide area. On the other hand, satellite images are very useful for grasping the damage situation over a wide area. In addition, satellite images include optical images and Synthetic Aperture Radar (SAR) image. During heavy rain, many clouds are generated. For this reason, many researches using SAR images which can observe day and night regardless of weather are carried out. However, the SAR image is complicated to operate and expensive, and it is not easy to use for users without expert knowledge. On the other hand, optical sensors can take images only in the clear daytime after the passing of rain cloud and typhoon, but it has the advantage that it is possible to obtain information in many bands, and that it is easy to decipher in comparison with SAR.

As the mentioned above, Shirozu et al. [1] and Honda et al. [2], tried to extract flooded areas from satellite images in order to evaluate damaged areas using SAR. Thus, many studies using SAR have been proposed. On the other hand, research using optical satellite images have been conducted by Sakuno [3] and Suhama et al. [4] However, it remains in the research of preliminary level due to the issues with filming conditions mentioned above.

Then, in this study, we focused on optical satellite images that are easy to process and intercept, and extracted the damaged area by combining existing methods such as a land cover classification method by machine learning and an additive color mixture.

2 SATELLITE IMAGE DATA

In order to extract the damaged areas from the satellite image, the satellite image of Landsat8 (30m resolution) were obtained from LandBrowser which a satellite data platform provided by the National Institute of Advanced Industrial Science and Technology (AIST). Satellite images before and after the disaster were prepared to extract the damaged areas from land cover changes caused by the disaster (Fig. 1). As a point to be noticed in analyzing the image in two different periods, the land cover in each season in the target areas is mentioned. For example, paddy fields are covered with water during the rice planting season, but there is no water in paddy fields in other seasons. Therefore, during the rice planting season, the area that is not originally water area may be determined to be water area by image analysis such as land cover classification. Since water level of paddy fields is managed seasonally, it is possible to prevent misclassification by using the data from the period when there is no water in the paddy field.

The study areas was Mabi-cho, Kurashiki City, Okayama Prefecture, which was severely damaged by 2018 Japan floods. Mabi-cho is surrounded by mountains. In Mabi-cho, houses and structures are comparatively few, and paddy field and croplands are widely distributed near the urban area. As shown in Fig. 1, the Takahashi River and Oda River run through the eastern part and the southern part of Mabi-cho, respectively. There are many water areas such as

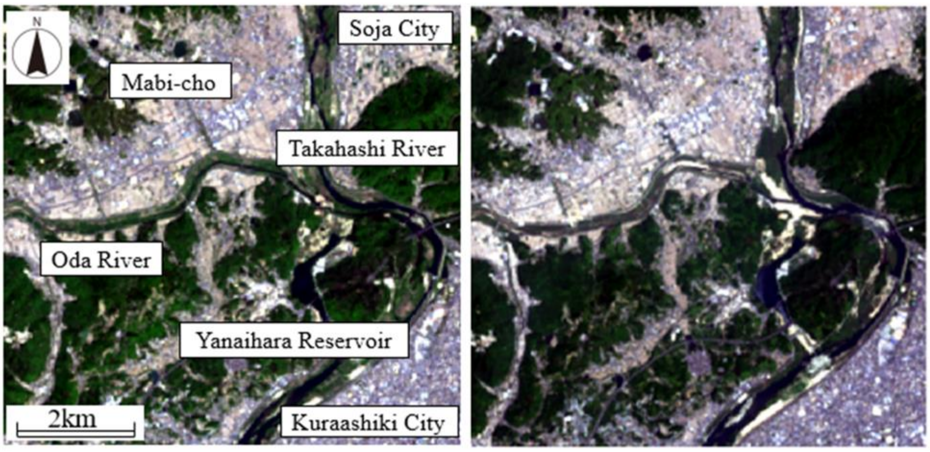

Fig. 1 Satellite image data (left : before the disaster, right : after the disaster)

reservoirs located near the Takahashi River. The dates of the used optical satellite images are as follows. As an image before the disaster, the image of April 20, 2018, taken on the closest to July 7, 2018, when the flooded damage in Mabi-cho reached its peak, is used, and as an image after the disaster, the image of May 25, 2019, about 10 months after the disaster occurrence day, is used. As for the image after the disaster, it is difficult to obtain the image taken in the day closet to the disaster occurrence day in LandBrowser due to the satellite's orbital position. Therefore, as noted above, in order to prevent misclassification, the images taken at the time closet to the day of disaster occurrence and with little seasonal effect were adopted.

3 IMAGE ANALYSIS METHOD

In this study, after land cover classification using a machine learning method for the optical images, an additive color mixture method is applied to the classified maps to extract the area where the land cover has changed.

3.1 Machine learning method

As a method to carry out the land cover classification, there is a technique called supervised classification in the machine learning method. Supervised classification is a method which applies supervised learning to image processing, and classifies specific geographical features included in an image using supervised data. Generally, if a geographical feature is known before classification, the feature data is classified as the training data. Among the supervised classification algorithms, the Maximum Likelihood (ML) method was used for land cover classification in this study.

The ML method expresses the feature values of geographical features to luminance value and variance of each band, and classifies these as training data. The following parameters are used to classify the objects into those with the maximum value (likelihood) as shown in Eq. 1. First, the luminance value in each band of the pixel to be classified. Second, the deviation matrix and the transposition matrix of the deviations calculated from the average luminance values in each band of the geographical feature. The third is the covariance-covariance matrix of the object and the inverse covariance-covariance matrix of the object. Likelihood is a function of the distribution of data in a category and is assumed to follow a normal distribution. In other words, it indicates the degree to which it is likely that certain data belong to a certain category.

To calculate the likelihood in the ML method, the features obtained from image pixels are represented by an n-dimensional vector x, where $x = [x_1,\ x_2,\ \cdots,\ x_n]$. Here n is the number of bands in the satellite image. An optical satellite image is a combination of several bands, and red, green, and blue bands are used for color display. Therefore, the number of bands is $n = 3$. The mean vector x of elements; $m = [m_1,\ m_2,\ \cdots,\ m_n]$, and the variance matrix is expressed in Eq. (1).

$$\Sigma = \begin{pmatrix} \sigma_{11}^2 & \cdots & \sigma_{1n}^2 \\ \vdots & \ddots & \vdots \\ \sigma_{n1}^2 & \cdots & \sigma_{nn}^2 \end{pmatrix} \tag{1}$$

lead to the following parameters. The vector of a classification category k is $x_k = [x_{k1},\ x_{k2},\ \cdots,\ x_{kn}]$, its mean vector is $m_k = [m_{k1},\ m_{k2},\ \cdots,\ m_{kn}]$, and its variance matrix is expressed in Eq. (2).

$$\Sigma_k = \begin{pmatrix} \sigma_{k11}^2 & \cdots & \sigma_{k1n}^2 \\ \vdots & \ddots & \vdots \\ \sigma_{kn1}^2 & \cdots & \sigma_{knn}^2 \end{pmatrix} \tag{2}$$

Assuming that the likelihood of unclassified image pixel x for classification category k is represented by normal distribution, the likelihood is calculated as in Eq. (3).

$$L(x,k) = \frac{1}{(2\pi)^{\frac{n}{2}}|\Sigma_k|^{\frac{1}{2}}} \exp\left\{-\frac{1}{2}d_M^2(x,k)\right\} \tag{3}$$

Here, $L(x,k)$ is the likelihood of data x for category k, $|\Sigma_k|$ is the variance-covariance matrix for category k, n is the number of bands (number of features), and $d_M^2(x,k)$ is the Mahalanobis Distance. The Mahalanobis Distance is the Euclidean Distance (Eq. (4)), which represents the distance between points in space, normalized by the variance-inverse matrix and expressed as Eq. (5).

$$d_E^2(x,k) = (x - m_k)(x - m_k)^t \tag{4}$$

$$d_M^2(x,k) = (x - m_k)\Sigma_k^{-1}(x - m_k)^t \tag{5}$$

Here, x is an n -dimensional vector, m_k is the mean vector of category k, $(x - m_k)$ is the deviation matrix, $(x - m_k)^t$ is the transpose matrix of the deviation, and Σ_k^{-1} is the variance-covariance inverse matrix for category k. That is, Eq. (3) can be rewritten as Eq. (6) using Eq. (5).

$$L(x,k) = \frac{1}{(2\pi)^{\frac{n}{2}}|\Sigma_k|^{\frac{1}{2}}} \exp\left\{-\frac{(x - m_k)\Sigma_k^{-1}(x - m_k)^t}{2}\right\} \tag{6}$$

However, in the actual classification process, the computational complexity is reduced as in Eq. (7) by taking the logarithm against the likelihood.

$$L'(x,k) = \ln(|\Sigma_k|) + \{(x - m_k)\Sigma_k^{-1}(x - m_k)^t\} \tag{7}$$

That is to say, the ML method is the technique by which the value obtained from the above equations is classified into the geographical features with the minimum [5,6].

3.2 Additive color mixture

The additive color mixture in image analysis is a method to confirm the image change by using the RGB value which expressed the image color, and by carrying out the addition processing of the pixel value for the image of two time period of red and cyan scaling. The colors represented in an image are called RGB values and are represented as (R, G, B) as shown in Fig. 2. In RGB values, red is represented as (255, 0, 0), green as (0, 255, 0), and blue as (0, 0, 255). Green + blue is cyan (0, 255, 255), red + green is yellow (255, 255, 0), and blue + red is purple (255, 0, 255). When all three colors are added the color is white (255, 255, 255), and when the color is represented by (0, 0, 0), the color is black.

In this study, we attempt to apply the additive color mixture to optical satellite images. Only the pixels that indicate the specific category in the land cover classification map are extracted and binarized. The same process is applied to both the image before and after the disasters and the result is added to the image to confirm for land cover changes based on the principle of additive color mixture. If there is no change in the geographical feature, it is represented as white; if red in the before image becomes black in the after image, it is expressed as red; conversely, if black in the before image becomes cyan in the after image, it is expressed as cyan; otherwise, it is expressed as black.

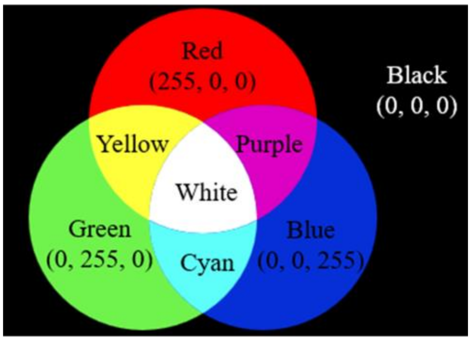

Fig. 2 Conceptual diagram of addtive color mixture

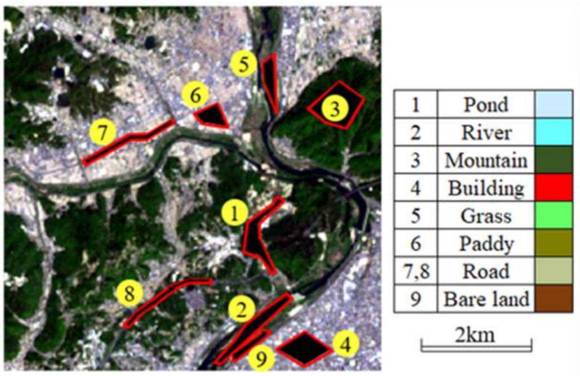

Fig. 3 Training data for classification

4 EXTRACTION OF DAMAGED AREA FROM SATELLITE IMAGE

4.1 Land cover classification using supervised classification

4.1.1 Training data

In order to conduct supervised classification, the training data is set in the areas indicated by the red frame in Fig. 3 for image before and after the disasters. The numbers in the legend on right side of Fig. 3 correspond to the numbers of yellow-colored circle in the figure. On the setting of each training data, the area indicating a specific category was selected visually on the satellite image. As has described above, the area is indicated by a red frame in Fig. 3. For example, in Fig. 3, a part of the image which is clearly a pond (1 of yellow-colored circle) is selected, and blue is assigned as a color indicating the pond. The same process was also carried

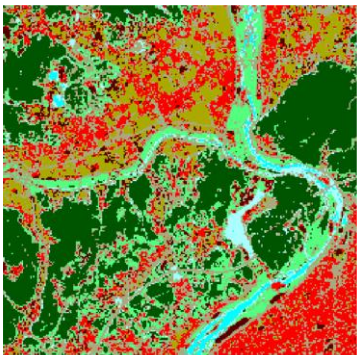

Fig. 4 Land cover classification (before the disaster)

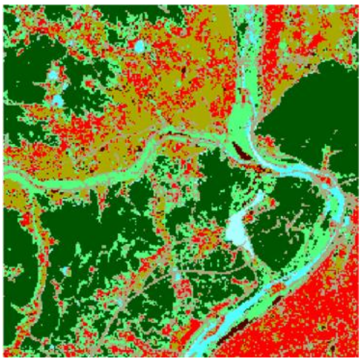

Fig. 5 Land cover classification (after the disaster)

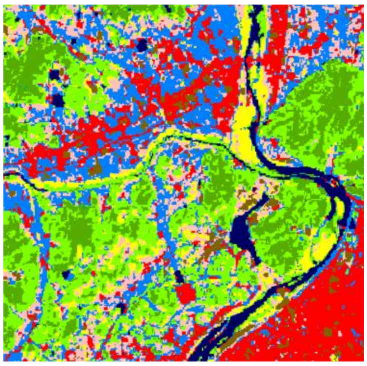

Fig. 6 Land cover classification (produced from JAXA)

out for the categories of river, mountain (vegetation), urban (building), grassland, paddy filed and cropland, road, and bare land. A total of eight categories of training data were created. For each category, colors were determined as follows so that land cover could be easily discriminated by color. The color was set as light blue for river, dark green for mountain (vegetation), red for urban (building), light green for grassland, olive for paddy field and cropland, light brown for road, and brown for bare land.

4.1.2 Land cover classification using image before the disaster

Fig. 4 shows the results of land cover classification by the above method for the satellite image (Fig. 1, left) before the disaster. First, the used satellite image (Fig. 1, left) and the results of land cover classification were visually deciphered to ensure that the geographical features were correctly classified. The water areas other than those set as the training data (region in the red flame indicated as 1 of yellow-colored circle in Fig. 2) are colored light blue, indicating that they were appropriately classified. For example, the Oda River, whose width is narrower than the Takahashi River, and the reservoirs scattered in the northern part of Mabi-cho as shown in light blue. Urban area with dense buildings is shown in gray color in the satellite image due to roof reflections. The area is classified by red, indicating buildings. As far as the coloring situation in Fig. 4 is concerned, the paddy filed or cropland and the buildings have different colors indicating that it is possible to classify them. However, regarding buildings and roads in urban area, the roads that are not adjacent to buildings (e.g., national roads) can be properly classified, but the roads adjacent to dense building area cannot be classified. In this study, we employed the expressway running east-west in the center of the satellite image and the national road running east-west in the urban area of Mabi-Cho as training data. The results showed that the roads set as the training data were properly classified, but the other two-lane roads were misclassified as the surrounding land cover which was classified into a different category from roads. From these results, it was proven that it is difficult to discriminate all two-lane roads using the satellite image of 30 m resolution adopted in this study. The reason of the misclassification can be attributed to the fact that many roads in rural area are not clearly divided into two laned (roads without a center line), and a single pixel in a low-resolution satellite image can contains multiple geographical features. Therefore, it is desirable to reduce the number of objects in a pixel to a single object.

Table 1 Confusion matrix

		Results						
		Water	Urban	Grass	Vegetation	Paddy Bare land	Tatal	PA(%)
Reference	Water	10010	62	508	140	3408	14128	70.9
	Urban	169	38252	409	64	18670	57564	66.5
	Grass	21	953	14753	1488	6597	23812	62.0
	Vegetation	664	330	25709	77419	10797	114919	67.4
	Paddy・Bare Land	0	18479	18597	1505	80088	118669	67.5
	Total	10864	58076	59976	80616	119560	329092	
	UA(%)	92.1	65.9	24.6	96.0	67.0		

4.1.3 Land cover classification of the image after the disaster

Fig. 5 shows the results of land cover classification by the above method for the satellite image (Fig. 1, right) after the disaster. The used satellite image (Fig. 1, right) and the results of land cover classification were visually deciphered to ensure that the geographical features were correctly classified. Regarding building and paddy field and cropland in the urban area can be properly classified as before the disaster, but the two-lane roads without a center line cannot be properly classified in some points. As for water area, the Oda River which flows south of Mabi-cho, is not classified as light blue. The reason for this is considered to be that the brown spots of the river were observed sporadically from the satellite image Fig. 1, that is, the earth and sand flowed into the river and the condition of the land cover become different. When it is difficult to accurately discriminate geographical features due to low resolution, misclassification can occur on land cover. From the above, it can be said that the classification of geographical feature below the resolution is difficult in both the images before and after disaster, but that other geographical feature can be classified as land cover in general.

4.1.4 Accuracy verification of land cover classification

An accuracy verification was conducted the land cover classification map in addition to visually deciphering. Compare the per-pixel RGB values of the land cover classification map and the reference data to see if they indicate the same geographical feature. As an image data (reference image data) used accuracy verification, a high-resolution land use and land cover map provided by the Japan Aerospace Exploration Agency (JAXA) was utilized (Fig. 6). The images taken by Landsat8 were also used for the land cover classification map prepared by JAXA as well as this study.

The discrimination efficiency table shown in Table 1 is prepared to verify the accuracy, and then the accuracy is evaluated by calculating the Overall Accuracy (OA). The OA is an accuracy evaluation index that indicates what percentage all pixels are correctly classified. The Producer's Accuracy (PA) and User's Accuracy (UA) were calculated in preparing the discrimination the confusion matrix. The PA is an index that indicates what percentage of the reference data is correctly classified, and the UA is an index that indicates what percentage of the classification results are correct. The OA of land cover classification map in this study was

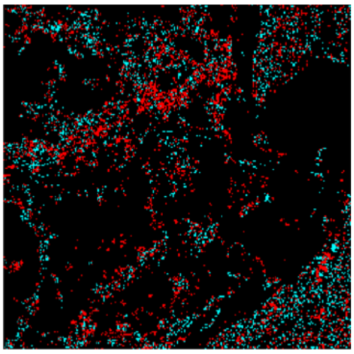

Fig. 7 Additive color mixture map (urban area)

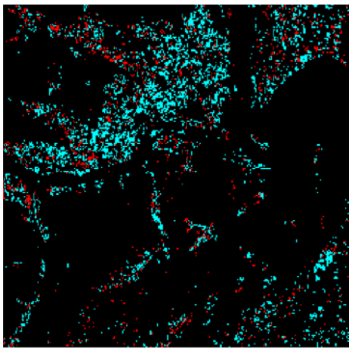

Fig. 8 Additive color mixture map (paddy field and cropland area)

calculated to be 67%. Thomlinson et al. [7] set a criterion of minimum of 85% for OA. This figure represents the accuracy standard for practical use of the land cover classification by Thomlinson et al. The results of this study were lower than the standard values. The reason why the value of OA is low is that the classification accuracy of grassland is especially low, which lowers the whole accuracy. As a reason why the classification accuracy of grassland become especially low, “low resolution of satellite image” is considered. The low resolution obscured the difference in color between grassland and mountains (vegetation), resulting in misclassification. By using higher resolution image, the difference in pixel color can be more clearly discriminated, and the frequency of misclassification may be reduced.

However, since the main objective of this study is to "extract the damaged areas," it is important to be able to confirm changes in land cover even at low resolution. Focusing on Mabi-cho, the land cover change (decrease in red pixels) can be visually confirmed. Therefore, in this study, the land cover change is captured by the additive color mixture method.

4.2 Result of image analysis using additive color mixture

By using the additive color mixture method for satellite image, only pixels corresponding specific categories are extracted. Then, binarization was conducted the image which was extracted the pixel, and the images before and after the disaster were added together. The areas that changed to white through the additive process were converted to black because cyan cannot be clarified when white and cyan coexist in the part changed to white due to contrast. In this paper, we present the following two categories that were most characterized by the additive color mixture method.

4.2.1 Urban area

First, Fig. 7 shows the results of applying additive color mixture to the image before the disaster (Fig. 4) and the image after the disaster (Fig. 5). Fig. 7 shows that red pixels are more distributed than cyan pixels over the entire region. This indicates that many of the buildings have disappeared for some reason between the two periods. Especially, when Mabi-cho is noticed, red pixels increase. Comparing with the flooded terrace map provided by the Geospatial Information Authority of Japan (GSI) [8], it is consistent with the flooded area by heavy rains. This indicates that most of the changes of buildings in Mabi-cho can be attributed to the disaster. It can be said that the method proposed in this study can classify the damaged areas appropriately.

4.2.2 Paddy field and cropland area

Fig. 8 shows the results of applying additive color mixture to the image before the disaster (Fig. 4) and the image after the disaster (Fig. 5) in the paddy field and cropland area as well as the urban area. In Fig. 8, there many cyan pixels as a whole, and it can be said that there are many geographical features classified as paddy field and cropland area after the disaster. In Mabi-cho, it is obvious. Especially, it is remarkable in the flooded area. It is considered that the buildings damaged by the disaster are not recognized as buildings because of the demolition, but as paddy fields and fields. It can be said that the reason why there are many cyan pixels indicating fields is also due to disasters. The result of the application of the additive color mixture to the paddy field and cropland area confirms that the number of buildings in Mabi-cho is decreasing due to the disaster.

4.2.3 Consideration

The above results show that the number of pixels indicating buildings decreased and the number of pixels indicating paddy field and cropland increased in the damaged areas. These areas correspond to the damaged areas. In this study, the relationship between land cover change in the urban area and the paddy field and cropland area enables us to easily identify the damaged areas. The satellite image data used in this study was taken after a certain period had passed since the disaster. However, if it is possible to obtain images immediately after the disaster, cyan pixels in the urban area of Mabi-cho can be more likely to appear in the result of additive color mixture. That is to say, after the disaster, it seems to be the result in which the wide area seems to be flooded. In such a case, the damaged areas would be extracted from the urban area and water area.

5 CONCLUSIONS

In this study, in order to extract the damaged area by the heavy rain disaster, the extraction of the damaged area was carried out by combining machine learning and image processing technology. To extract the damaged area, the land cover classification by machine learning was carried out, and the additive color mixture method was applied to the classified maps, followed by additive processing. As a result of the application, it become possible to visually represent the land cover changes before and after the disaster in specific categories and to extract the damaged areas.

This study is positioned as basic research on the extraction of damaged areas immediately after a disaster. On the other hand, it is necessary to pay attention to issues such as low resolution for practical application. In the future, the examination for the practical application should be carried out using the image with high resolution in order to improve the accuracy of land cover classification.

ACKNOWLEDGMENT

This work was supported by A General Incorporated Association Shikoku Create. We express our gratitude here.

REFERENCES

[1] Hajime, S., Kaiki, K., Haruhiko, Y. and Koji, A. *Study on Estimation Method of Inundation Area and Depth Using SAR Data*. Jounal of Japan Society of Civil Engineers, Ser. B1(Hydraulic Engineering), Vol.75, No.2, I_1471-I_1476, 2019

[2] Kenichi, H., Yusuke, I., Keita, H., Naruo, M., Norichika, A. and Koichi, T. *A Study on Rapid Estimation of Inundation Area and Flood Depth during Heavy Rain Disaster Using Satellite SAR*. Journal of The Remote Sensing Society of Japan, Vol.40, No.3, pp.158-162, 2020

[3] Yuji, S., *Flooded Area Estimation Using Landsat-8 and Sentinel-1 after the Heavy Rain Disaster in the Western Japan*. Journal of The Remote Sensing Society of Japan, Vol.38, No.5, pp.435-437, 2018

[4] Tomoyuki, S., Yuya, F., Akihisa, I., Tomoyuki, K. and Tomohiro, H. *Satellite Observation by AIRBUS DS and MDA for Torrential Rains in Western Japan*. Journal of The Remote Sensing Society of Japan, Vol.38, No.5, pp.431-434, 2018

[5] Shafri, H.Z.M., Suhaili, A., Mansor, S. *The performance of maximum likehood, spectral angle mapper, neural network and decision tree classifiers in hyperspectral image analysis*, Journal Computer Science, Vol.3, pp.419-423, 2007

[6] Harumi, I. and Minoru, I. *Classification Tendency Analysis of the Land Cover Category Classification Methods Using Multispectral Image Data*. Journal of The Remote Sensing Society of Japan, Vol.23, No.2, pp.126-136, 2003

[7] Thomlinson, J.R., V Bolstad, P. and Cohen, W.B. *Coordinating Methodologies for Scaling Landcover Classifications from Site Specific to Global*, Remote Sensing of Environment, Vol.70, No.1, pp.16-28, 2007

[8] Geospatial Information Authority of Japan (2018), "Information on heavy rain in western Japan", https://www.gsi.go.jp/BOUSAI/H30.taihuu7gou.html, 31, May, 2022